RESULTS OF THE FIRST INTERFEROMETRIC MEASUREMENTS OF UNDULATOR RADIATION FROM SINGLE ELECTRONS*

G. Stancari†, J. Jarvis, A. Romanov, A. Shemyakin, A. Valishev
Fermi National Accelerator Laboratory, Batavia, IL, United States
I. Lobach, S. Nagaitsev, Brookhaven National Laboratory, Upton, NY, United States

Abstract

The aims of the CLARA experiment at the Fermilab Integrable Optics Test Accelerator (IOTA) were to directly measure the coherence length of undulator radiation emitted by a single electron and to test whether the radiation is in a pure classical Glauber coherent state or in a quantum mixture of coherent and Fock states. We used a Mach-Zehnder interferometer (MZI) to study visible radiation generated by 150-MeV electrons circulating in the ring. The relative delay between the two arms of the MZI was adjusted by varying the length of one of them with a resolution of 10 nm. The intensity of the circulating beam spanned several orders of magnitude, down to single electrons. A pair of single-photon avalanche diodes (SPADs) was placed at the output of the MZI arms to detect photocounts with high efficiency and timing resolution. We describe the observed interference patterns and photocount rates as a function of interferometer delay. The arrival time distributions of photocounts of undulator radiation, lasers and chaotic light are compared. The implications for the quantum-optical nature of the radiation are discussed. To our knowledge, these are the first direct measurements of this kind.

INTRODUCTION

Synchrotron-radiation sources have had an immense impact on many scientific fields. The same is true for sources of well-defined quantum states of radiation [1, 2]. At Fermilab, using the Integrable Optics Test Accelerator (IOTA) [3], we are carrying out an experimental program to study the classical and quantum properties of undulator radiation from electron bunches and from individual electrons [4]. We are addressing the following scientific questions: What are the properties of radiation from single electrons? Can one directly observe the classical or quantum nature of undulator radiation? We are also interested in new ways to generate quantum states of light and in novel applications of the experimental techniques of quantum optics in accelerator physics and beam diagnostics.

Classical electrodynamics explains a wide range of phenomena: reflection and refraction, interference, diffraction, synchrotron radiation, etc. The theory of quantum optics [5–12] offers a deeper understanding of the nature of radiation and is necessary to explain physical observations such as spontaneous emission, the Lamb shift and the Hong-Ou-Mandel effect [13], for instance. In quantum optics, physical systems are described by different quantum states of radiation. Classical waves, such as those generated by dipole antennas or lasers, are represented by Glauber coherent states. Radiation from individual atoms, parametric down-conversion or quantum dots, on the other hand, corresponds to Fock number states. The properties of thermal or chaotic sources of light, such as light bulbs, black bodies or stars, are represented by incoherent mixtures of states via the density-matrix formalism. Experimentally, states can be identified by observing the statistics of photocounts, such as intensity fluctuations or arrival-time distributions. With multiple photodetectors, one can also study coincidence rates. For instance, Hong, Ou and Mandel observed that when radiation is in a 2-photon number state, coincidences are suppressed [13]. When the energy of the radiation (~eV) is small compared to the energy of the radiating particle (150-MeV electrons, in our case), radiation is expected to be in a coherent state, behaving like a classical wave even when it is emitted by a single electron [14].

It is interesting to note that testing the coherent-state description of a radiation field may in the future be related to the experimental investigation of quantum gravity, following the suggestion that graviton detection sensitivity may be reached with quantum sensors [15, 16].

Radiation from single electrons has been studied in the past [17–19]. Recently, for instance, the techniques of quantum optics were applied to the study of radiation in a tandem undulator [20] and a free-electron laser [21].

In previous experiments [22–25], we verified that intensity fluctuations in undulator radiation contain, in addition to a Poissonian term, a calculable term which depends on beam sizes. Beam emittances can therefore be inferred from intensity fluctuations. With a single photodetector, we observed that photocount statistics was consistent with a coherent state of radiation. Arrival-time distributions were used to measure jitter in the radiofrequency accelerating cavities and to estimate bunch lengths at the smallest beam intensities. The CLARA experiment in IOTA Run 4 (2022–2023) [26] used a Mach-Zehnder interferometer (MZI) to directly measure the coherence length of undulator radiation from single electrons and to study photocount statistics. Preliminary results were presented in Ref. [27]. Here, we present the interferometry results on coherence length measurements and discuss some of the observations of photocount statistics.

* This manuscript has been authored by Fermi Forward Discovery Group, LLC under Contract No. 89243024CSC000002 with the U.S. Department of Energy, Office of Science, Office of High Energy Physics. Work partially supported by the University of Chicago Consortium for Advanced Science and Engineering (CASE). Report No. FERMILAB-CONF-26-0126-AD.

† stancari@fnal.gov

EXPERIMENTAL METHODS

Electrons were stored in IOTA at 150 MeV in a single bunch. The revolution period was 133 ns. Beam intensities were varied between the nominal injection charge (~ 10^9 electrons or 1.2 mA) down to a single electron. Single electrons were obtained by detuning injection of dark current from the superconducting linac or by controlled scraping with lowered radiofrequency (rf) cavity voltages. Intensities were monitored with a current transformer in the upper range and with synchrotron-radiation photomultipliers and digital cameras over the whole range.

The undulator [28] was installed in one of the IOTA straight sections (Fig. 1). It had 10.5 periods with length λ_u = 55 mm each. The gap was tuned to the undulator parameter K_u = 1.06. The experiment was originally designed to run at 135 MeV, to match the first harmonic of undulator radiation λ_1 = 611 nm to the photodetectors (described below). For practical reasons and for compatibility with the concurrent studies on nonlinear integrable optics, it was decided to run at 150 MeV with λ_1 = 495 nm, with a ~40% loss of detection efficiency.

The Mach-Zehnder interferometer was installed on top of the dipole magnet downstream of the undulator (Fig. 1). Undulator radiation was collected by a periscope containing two adjustable mirrors and a variable iris. The light beam was projected onto the flipping screen FS and observed through the webcam C (image with colored rings in Fig. 1). When the screen FS was retracted, the light was focused by lens LS0 and injected into the interferometer's first 50:50 beam splitter (BS1). In arm 1, light was directed by mirrors IM1 and IM2 to a second identical beam splitter (BS2). The horizontal and vertical angular positions of IM1 and BS2 were controlled by closed-loop picomotors. In arm 2, light was either intercepted by the flipping screen FA2 or directed by the right-angle mirror IM3 and by the hollow-roof mirror IM4 to the beam splitter BS2. The difference in propagation times (delay) between the two arms was adjusted by changing the position of IM4. This mirror was mounted on a precision translation stage with minimum steps of 20 nm. The output beams of beam splitter BS2 were directed through focusing lenses LS1 and LS2 toward 2 single-photon avalanche diodes (SPADs), with 0.18-mm-diameter active area. When the flipping mirror FM was inserted, the light from one of the output ports was sent to the digital camera DC (interference pattern at top right of Fig. 1). Each SPAD could be aligned longitudinally, horizontally and vertically. To reduce vibrations, the interferometer was assembled on a separate breadboard. For alignment and commissioning, 635-nm light from a laser diode (LD) was injected at the second input of beam splitter BS1.

The SPAD signals were monitored on an oscilloscope and sent to the data-acquisition chain. Data included raw counts, detector rates and coincidence rates, recorded at 15 Hz. For the continuous laser diode light source, the coincidence window was typically 20 ns. When observing pulsed radiation from the circulating electron beam, the coincidence window was a full 133-ns turn, with the option to define a gate of 10 ns around the bunch arrival time. The standard deviation of the bunch length was 0.7 ns. Time-tagged photocounts were also acquired with an event timer, which had a resolution of 1 ps and an accuracy of 15 ps. This allowed us to analyze photocounts and coincidences offline, with programmable gating and coincidence window settings.

In a typical experiment, electrons were injected in IOTA at full intensity. The beam was then moved from the injection to the central orbit. The periscope mirrors were adjusted to align the light beam with the center of the iris and of the camera. The lengths of the MZI arms were equalized to find the interference condition. The light beam angles were aligned by observing fringe visibility on the digital camera. The beam was then scraped to hundreds of electrons by reducing the voltage in the rf cavity. At this point, it was safe to turn on the SPADs and to check their alignment. Data were then collected under various conditions, such as number of electrons, MZI arm delay and iris opening.

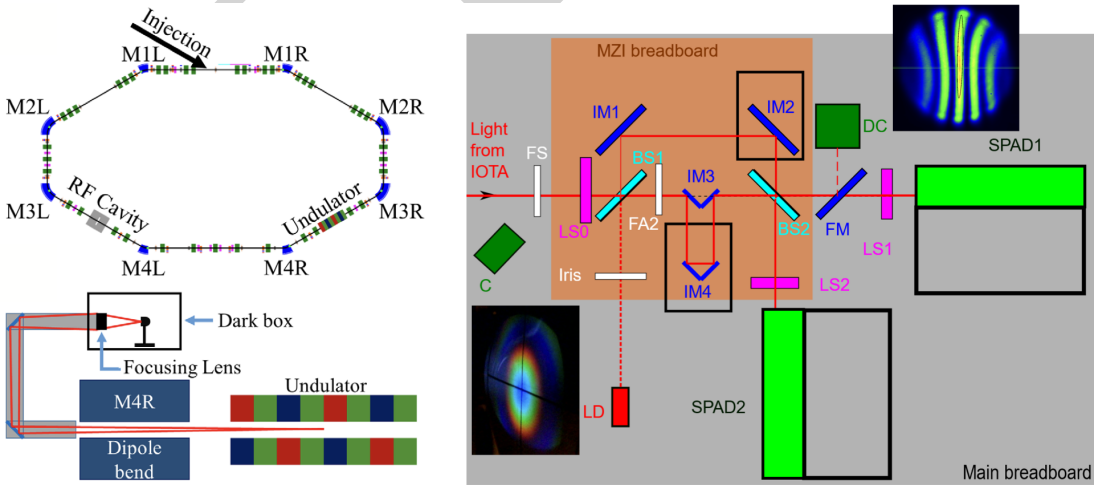

Figure 1: Schematic diagram of the apparatus. (left, top) Undulator location in the IOTA ring. (left, bottom) Light collection from the undulator to the dark box on top of the M4R dipole magnet. (right) The Mach-Zehnder interferometer.

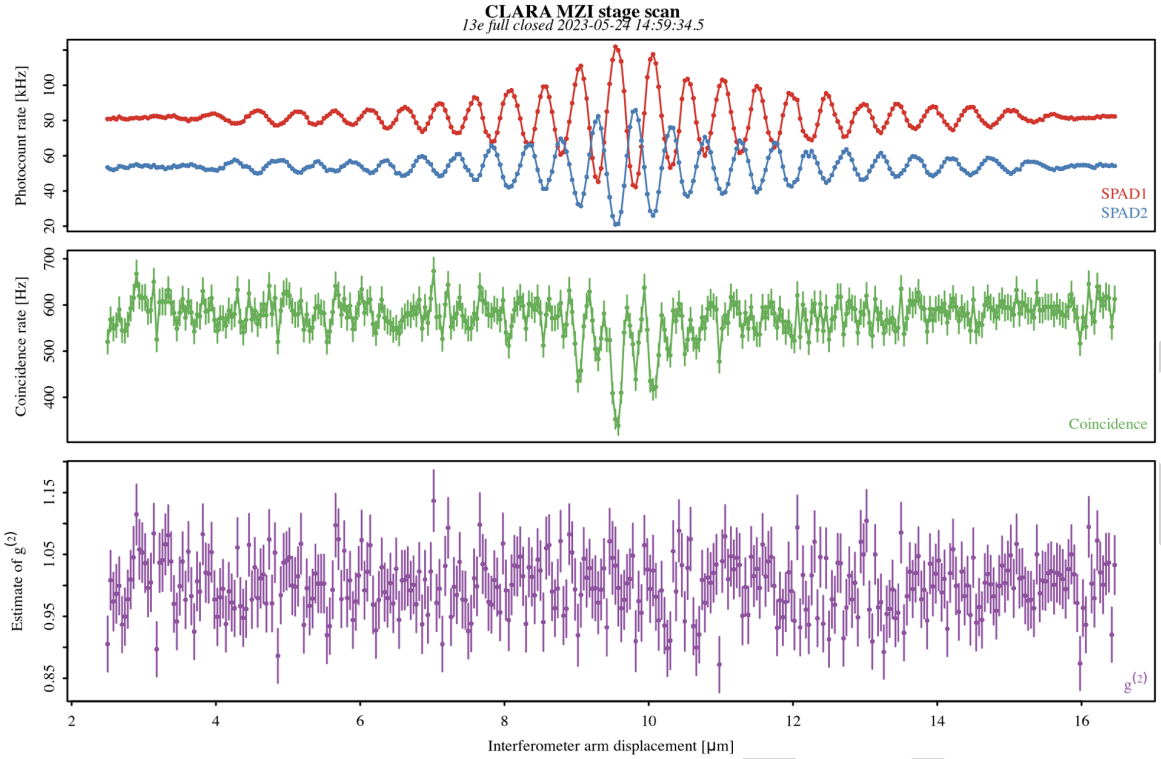

Figure 2: Detector and coincidence rates vs. arm length for a full delay scan with 13 electrons circulating in the IOTA ring and narrow iris aperture.

ANALYSIS AND RESULTS

Temporal Coherence

During an optical delay scan, photocount rates R_1 and R_2 in each detector and in coincidence R_c were recorded as a function of the interferometer arm delay x. The longitudinal coherence length L_c or coherence time $\tau_c = L_c/c$ of the radiation were estimated from the resulting interference pattern. Figure 2 shows the detector and coincidence rates as a function of arm length. In this scan, data were taken for 1 s at each of the 350 20-nm steps. Several other scans were taken with different numbers of electrons, acquisition times and iris aperture settings (to select different spectral ranges of the incoming radiation). An example of interferogram for a single detector is shown in Fig. 3. It was taken with 1 electron in IOTA.

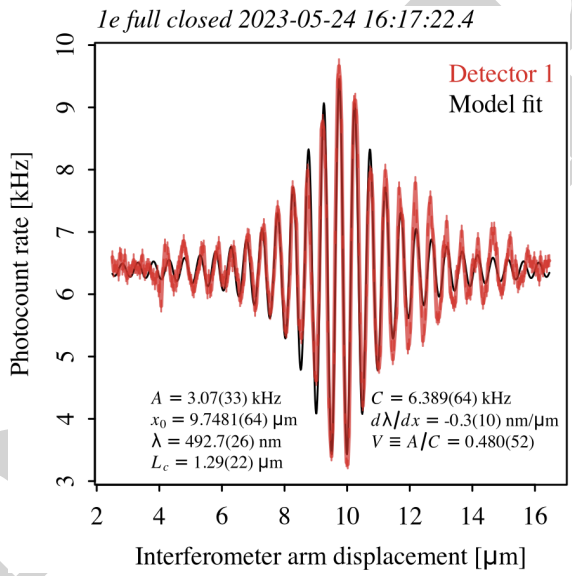

Figure 3: Example of interferogram data and corresponding model fit. The delay scan was done with 1 circulating electron and narrow iris aperture.

To estimate the coherence length, the interference pattern is modeled as a sinusoid of amplitude A with a Lorentzian envelope, plus a constant level C:

$$R(x) = A\frac{\cos\left[2\pi(x-x_0)/\lambda'\right]}{1+\left[(x-x_0)/L_c\right]^2} + C$$
$$\lambda' = \lambda + \left(\frac{d\lambda}{dx}\right)(x-x_0). \quad (1)$$

We use the half width at half maximum (HWHM) of the Lorentzian shape as estimate of the coherence length L_c. The maximum visibility of the interference fringes is $V = A/C$. Because the radiation is not monochromatic, we allow the wavelength λ' to vary linearly with displacement by a small amount, $(d\lambda/dx) \sim 1$ nm/μm. This also accounts for uncertainties in the calibration of the delay stage. All measured interferograms are fitted with this model to extract the 6 parameters A, x_0, λ, L_c, C and $(d\lambda/dx)$ and their uncertainties. Of course, the shape of the envelope depends on the spectrum of the radiation. The model is not expected to reproduce the interferogram exactly. However, the estimates of coherence length are quite robust.

A complementary perspective on coherence is given by the spectral analysis of interferograms. The width of the frequency spectrum is inversely proportional to the coherence time. Figure 4 shows the Fourier spectrum of 3 interferograms. The blue one and the green one were both taken with a narrow iris aperture, limiting the radiation to the cyan region of the spectrum, as can also be seen qualitatively in the screen image of Fig. 1. No appreciable difference is observed between the spectrum from 13 electrons (blue) and from 1 electron (green). The pink spectrum was taken with 1 electron and a wide iris aperture. One can see a considerable widening of the range of wavelengths.

Because the spectra are often irregular or asymmetric, the coherence length is roughly estimated from the inverse of the interquartile range of the distribution of spatial frequencies f: $L_c \simeq (1/2) \cdot 1/(f_{75\%} - f_{25\%})$. These estimates are consistent with the ones from the interferogram model fit, but are less accurate.

A summary of the coherence length measurements is shown in Fig. 5 as a function of the number of circulating electrons and of iris setting. The error bars indicate statistical uncertainties. Systematic uncertainties are of the order of 0.1 µm. Measurements for different numbers of electrons, from 1 to 300, are consistent. When the iris is opened to its wide setting, the coherence length drops from 1.4 µm to 1.0 µm. These measurements indicate that, with interferometric techniques, coherence times of undulator radiation can be directly measured with femtosecond sensitivity.

Photocount Statistics

The value of the coincidence rate near the interference condition with respect to its value away from interference gives information about the nature of the radiation.

For randomly distributed events, the coincidence rate in a time window t_w is $R_c = R_1 \cdot R_2 \cdot t_w$. From the measured detector and coincidence rates, using a known coincidence window, one can estimate the degree of second-order coherence $g^{(2)}$ of the radiation. For comparisons with experiments, we define a normalized coincidence rate $r_c \equiv R_c/(R_1 \cdot R_2 \cdot t_w) \simeq g^{(2)}$. For classical radiation (coherent states), $r_c = 1$. For thermal radiation, $r_c \geq 1$. For quantum states of light with no classical analogue, such as a 2-photon number states, $r_c < 1$.

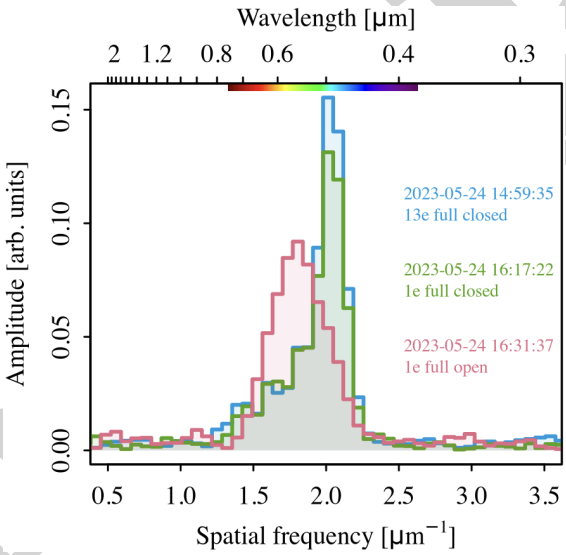

Figure 4: Comparison of interferogram spectra for 3 data sets: 13 electrons, narrow iris (blue); 1 electron, narrow iris (green); 1 electron, wide iris (pink).

Two main effects can influence the value of the normalized coincidence rate: mechanical vibrations and background counts. Mechanical vibrations generate fluctuations in the lengths of the interferometer arms, which result in a reduction of coincidence rates near the center of the interference pattern, mimicking a Hong-Ou-Mandel dip. Vibrations were studied and mitigated. Their effect on coincidences was reduced to the level of 1% [29]. If the observed signal is the sum of the photodetector rate of interest plus a known background rate, $S_1 = R_1 + B_1$ and $S_2 = R_2 + B_2$, then the actual coincidence rate can be estimated by correcting the observed coincidence rate: $R_1R_2 = S_1S_2 - S_1B_2 - B_1S_2 + B_1B_2$. Background rates were often negligible, but not always, especially at low electron beam currents. We also found that the SPAD dark count rates could change significantly over time. Backgrounds were measured with no beam and with detector shutters closed. They were also significantly reduced by gating photocounts around the arrival time of the bunch, as described above.

An example of the evolution of the raw and normalized coincidence rates during a stage scan can be seen in Fig. 2. In the case of light from the laser diode, we observed changes in the normalized coincidence rate and in the time structure of coincidences as a function of the diode current, as the device transitioned from thermal light and spontaneous emission to stimulated emission and lasing. In the case of undulator radiation, the normalized coincidence rate is constant and consistent with $r_c = 1$ (purple data in Fig. 2, for instance). For the case of single electrons, we took high-statistics scans (100 s per point). The data suggest that undulator radiation, even for single electrons, is in a pure coherent state. A detailed analysis of coincidences will be published in a separate report.

CONCLUSIONS

Through interferometry of undulator radiation from single electrons and from known numbers of electrons, we directly observed the temporal coherence at the femtosecond scale. Preliminary results are consistent with radiation in a coherent state. The techniques of quantum optics have already yielded novel and sensitive diagnostics tools. Further examples may include investigations of the physics of optical stochastic cooling [30] or the measurement of small beam sizes based on the Hanbury Brown and Twiss effect, analogous to stellar interferometry [31]. In a storage ring, it may be possible to generate tagged radiation in specific quantum states, as in the Compton scattering of stored electrons with thermal photons [32, 33].

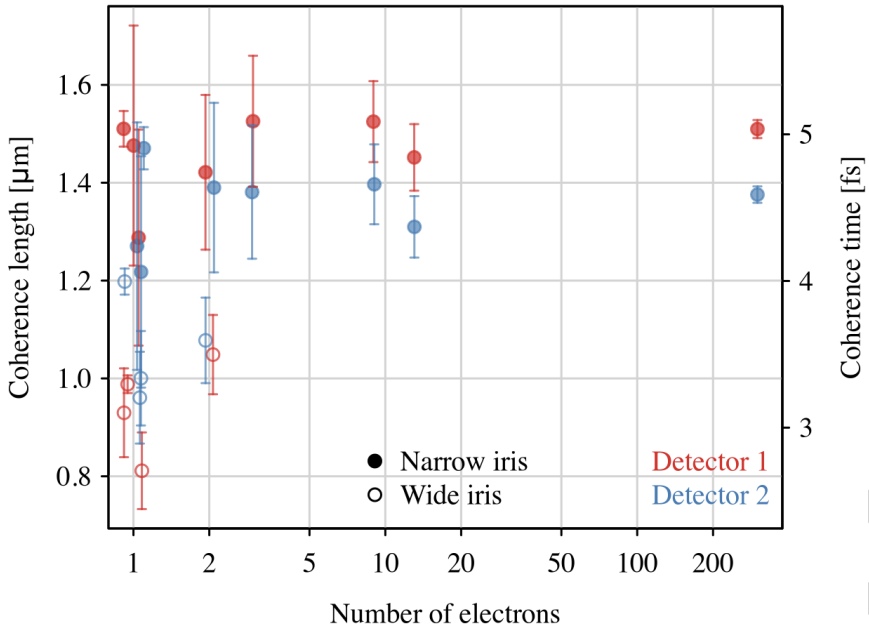

Figure 5: Coherence lengths and corresponding coherence times estimated from interferograms, for data sets with different numbers of electrons and iris apertures.

ACKNOWLEDGMENTS

We would like to thank the members of the IOTA/FAST group at Fermilab for making these experiments possible, in particular D. Broemmelsiek, D. Edstrom, D. MacLean, J. Ruan, J. Santucci, and T. Thompson. Special thanks to Zhirong Huang (SLAC) for his support and for providing the undulator.

REFERENCES

[1] C. Couteau *et al.*, "Applications of single photons to quantum communication and computing", *Nat. Rev. Phys.*, vol. 5, no. 6, pp. 326–338, 2023. doi:10.1038/s42254-023-00583-2

[2] C. Couteau *et al.*, "Applications of single photons in quantum metrology, biology and the foundations of quantum physics", *Nat. Rev. Phys.*, vol. 5, no. 6, pp. 354–363, 2023. doi:10.1038/s42254-023-00589-w

[3] S. Antipov *et al.*, "IOTA (Integrable Optics Test Accelerator): facility and experimental beam physics program", *J. Instrum.*, vol. 12, no. 03, T03002, Mar. 2017. doi:10.1088/1748-0221/12/03/t03002

[4] S. Nagaitsev, I. Lobach, A. Romanov, and G. Stancari, "Quantum effects in undulator radiation", Fermilab LDRD Grant no. L2019.025, June 2019 – March 2023, Jun. 2019,

[5] R. J. Glauber, "Some notes on multiple-boson processes", *Phys. Rev.*, vol. 84, no. 3, p. 395, 1951. doi:10.1103/PhysRev.84.395

[6] R. J. Glauber, "Coherent and incoherent states of the radiation field", *Phys. Rev.*, vol. 131, no. 6, p. 2766, 1963. doi:10.1103/PhysRev.131.2766

[7] R. J. Glauber, "The quantum theory of optical coherence", *Phys. Rev.*, vol. 130, no. 6, p. 2529, 1963. doi:10.1103/PhysRev.130.2529

[8] R. J. Glauber, "Nobel lecture: one hundred years of light quanta", *Rev. Mod. Phys.*, vol. 78, no. 4, pp. 1267–1278, 2006. doi:10.1103/RevModPhys.78.1267

[9] L. Mandel and E. Wolf, *Optical coherence and quantum optics*. Cabridge, UK: Cambridge University Press, 1995. doi:10.1017/CBO9781139644105

[10] R. Loudon, *The quantum theory of light*. Oxford Science Publications, 2000.

[11] G. Grynberg, A. Aspect, and C. Fabre, *Introduction to quantum optics: from the semi-classical approach to quantized light*. Cambridge, UK: Cambridge University Press, 2010. doi:10.1017/CBO9780511778261

[12] H.-A. Bachor and T. C. Ralph, *A guide to experiments in quantum optics*. Hoboken, NJ, USA: Wiley, Sep. 2019. doi:10.1002/9783527695805

[13] C. K. Hong, Z. Y. Ou, and L. Mandel, "Measurement of subpicosecond time intervals between two photons by interference", *Phys. Rev. Lett.*, vol. 59, no. 18, pp. 2044–2046, Nov. 1987. doi:10.1103/PhysRevLett.59.2044

[14] F. Bloch and A. Nordsieck, "Note on the radiation field of the electron", *Phys. Rev.*, vol. 52, no. 2, pp. 54–59, 1937. doi:10.1103/PhysRev.52.54

[15] G. Tobar, S. K. Manikandan, T. Beitel, and I. Pikovski, "Detecting single gravitons with quantum sensing", *Nat. Commun.*, vol. 15, no. 1, p. 7229, 2024. doi:10.1038/s41467-024-51420-8

[16] S. K. Manikandan and F. Wilczek, "Testing the coherent-state description of radiation fields", *Phys. Rev. A*, vol. 111, no. 3, p. 033705, 2025. doi:10.1103/PhysRevA.111.033705

[17] I. A. Grishaev, N. N. Naugolnyi, L. V. Reprintsev, A. S. Tarasenko, and A. M. Shenderovich, "Interference experiment and photon statistics for synchrotron radiation from electrons in a storage ring", *Sov. Phys. JETP*, vol. 32, no. 1, pp. 16–19, 1971.

[18] I. A. Grishaev, I. S. Guk, A. S. Mazmanishvili, and A. S. Tarasenko, "Interference of synchrotron radiation photons from a single electron", *Sov. Phys. JETP*, vol. 36, no. 5, pp. 870–871, 1973.

[19] I. V. Pinayev, V. M. Popik, T. V. Shaftan, A. S. Sokolov, N. A. Vinokurov, and P. V. Vorobyov, "Experiments with undulator radiation of a single electron", *Nucl. Instrum. Methods Phys. Res. A*, vol. 341, pp. 17–20, Mar. 1994. doi:10.1016/0168-9002(94)90308-5

[20] T. Kaneyasu *et al.*, "Double-pulsed wave packets in spontaneous radiation from a tandem undulator", *Sci. Rep.*, vol. 12, no. 1, p. 9682, Dec. 2022. doi:10.1038/s41598-022-13684-2

[21] Y. Y. Kim *et al.*, "Statistical analysis of hard x-ray radiation at the PAL-XFEL facility performed by Hanbury Brown and Twiss interferometry", *J. Synchrotron Rad.*, vol. 29, no. 6, pp. 1465–1479, Nov. 2022. doi:10.1107/S1600577522008773

[22] I. Lobach *et al.*, "Statistical properties of spontaneous synchrotron radiation with arbitrary degree of coherence", *Phys. Rev. Accel. Beams*, vol. 23, no. 9, p. 090703, Sep. 2020. doi:10.1103/PhysRevAccelBeams.23.090703

[23] I. Lobach *et al.*, "Measurements of undulator radiation power noise and comparison with ab initio calculations", *Phys. Rev. Accel. Beams*, vol. 24, no. 4, p. 040701, Apr. 2021. doi:10.1103/PhysRevAccelBeams.24.040701

[24] I. Lobach *et al.*, "Transverse beam emittance measurement by undulator radiation power noise", *Phys. Rev. Lett.*, vol. 126, no. 13, p. 134802, Apr. 2021. doi:10.1103/PhysRevLett.126.134802

[25] I. Lobach, S. Nagaitsev, A. Romanov, and G. Stancari, "Single electron in a storage ring: a probe into the fundamental properties of synchrotron radiation and a powerful diagnostic tool", *J. Instrum.*, vol. 17, no. 2, P02014, Feb. 2022. doi:10.1088/1748-0221/17/02/P02014

[26] S. Nagaitsev *et al.*, "Measurement of coherence length in undulator radiation (CLARA): run 4 proposal", Fermilab, Batavia, IL, USA, Rep. FERMILAB-TM-2804-AD, Sep. 2023. doi:10.2172/1997543

[27] G. Stancari *et al.*, "Undulator radiation of single electrons: coherence length and quantum-optical properties", in *Proc. IPAC'24*, Nashville, TN, USA, pp. 300–303, Jul. 2024. doi:10.18429/JACoW-IPAC2024-MOPG06

[28] S. C. Gottschalk, R. N. Kelly, M. A. Offenbacker, and J. F. Zumdieck, "Design and performance of the NLCTA-Echo 7 undulators", in *Proc. FEL'12*, Nara, Japan, paper THPD12, pp. 571–574, Aug. 2012. https://jacow.org/FEL2012/papers/THPD12.pdf

[29] G. Stancari, A. Shemyakin, and A. Romanov, "Vibration studies for the CLARA interferometer", Fermilab, Batavia, IL, USA, Rep. FERMILAB-FN-1246-AD, May 2024. doi:10.5281/zenodo.14897588

[30] J. Jarvis *et al.*, "Experimental demonstration of optical stochastic cooling", *Nature*, vol. 608, no. 7922, pp. 287–292, Aug. 2022. doi:10.1038/s41586-022-04969-7

[31] R. Hanbury Brown and R. Q. Twiss, "A test of a new type of stellar interferometer on Sirius", *Nature*, vol. 178, no. 4541, pp. 1046–1048, Nov. 1956. doi:10.1038/1781046a0

[32] V. I. Telnov, "Scattering of electrons on thermal radiation photons in electron-positron storage rings", *Nucl. Instrum. Methods Phys. Res. A*, vol. 260, pp. 304–308, Oct. 1987. doi:10.1016/0168-9002(87)90093-3

[33] B. Dehning, A. C. Melissinos, F. Perrone, C. Rizzo, and G. von Holtey, "Scattering of high energy electrons off thermal photons", *Phys. Lett. B*, vol. 249, no. 1, pp. 145–148, Oct. 1990. doi:10.1016/0370-2693(90)90540-M